

Kinetic modelling and mechanism of dye adsorption on unburned carbon

Shaobin Wang*, Huiting Li

Department of Chemical Engineering, Curtin University of Technology, GPO Box U1987, Perth, WA 6845, Australia

Received 11 May 2005; received in revised form 19 July 2005; accepted 2 September 2005

Available online 24 October 2005

Abstract

Textile dyeing processes are among the most environmentally unfriendly industrial processes by producing coloured wastewaters. The adsorption method using unburned carbon from coal combustion residue was studied for the decolourisation of typical acidic and basic dyes. It was discovered that the unburned carbon showed high adsorption capacity at 1.97×10^{-4} and 5.27×10^{-4} mol/g for Basic Violet 3 and Acid Black 1, respectively. The solution pH, particle size and temperature significantly influenced the adsorption capacity. Higher solution pH favoured the adsorption of basic dye while reduced the adsorption of acid dye. The adsorption of dye increased with increasing temperature but decreased with increasing particle size. Sorption kinetic data indicated that the adsorption kinetics followed the pseudo-second-order model. The adsorption mechanism consisted of two processes, external diffusion and intraparticle diffusion, and the external diffusion was the dominating process. © 2005 Elsevier Ltd. All rights reserved.

Keywords: Unburned carbon; Dye adsorption; Kinetics; Adsorption isotherm

1. Introduction

Dyes are a kind of organic compounds with a complex aromatic molecular structure that can bring bright and firm colour to other substances. However, the complex aromatic molecular structures of dyes make them more stable and more difficult to biodegrade. The extensive use of dyes often poses pollution problems in the form of coloured wastewater discharged into environmental water bodies [1,2]. One of the conventional methods for removal of dyes from wastewater is adsorption [3–5]. Activated carbon is popular and an effective dye sorbent, but its relatively high price, high operating costs and problems with regeneration hamper its large-scale application. Therefore, there is a growing need in finding low cost, renewable, locally available materials as sorbent for the removal of dye colours [3,5].

Unburned carbon is one of the important components in coal combustion residue, fly ash. High carbon content in fly

ash results in the less application of fly ash for cement production. However, due to the high-temperature treatment, unburned carbon could have been developed with good porosity [6–8]. The unburned carbon in fly ash thus could be a good adsorbent and precursor for production of activated carbon [9]. Utilisation of unburned carbon could bring out enormous economic and environmental benefits to the coal and utility industries. Fly ash has been recently employed as a cheap adsorbent for dye adsorption [5,10–14]. However, few investigations have reported on unburned carbon as effective adsorbents. Our investigation discovered that unburned carbon made a significant contribution to adsorption capacity of fly ash in dye removal [7]. The aim of this study is to further explore the application of unburned carbon for dye adsorption and to investigate the kinetics and mechanism involved in dye adsorption on unburned carbon.

2. Experimental

Unburned carbon was obtained by separation of fly ash using a two-step method. Firstly, the raw fly ash was sieved

* Corresponding author.

E-mail address: wangshao@vesta.curtin.edu.au (S. Wang).

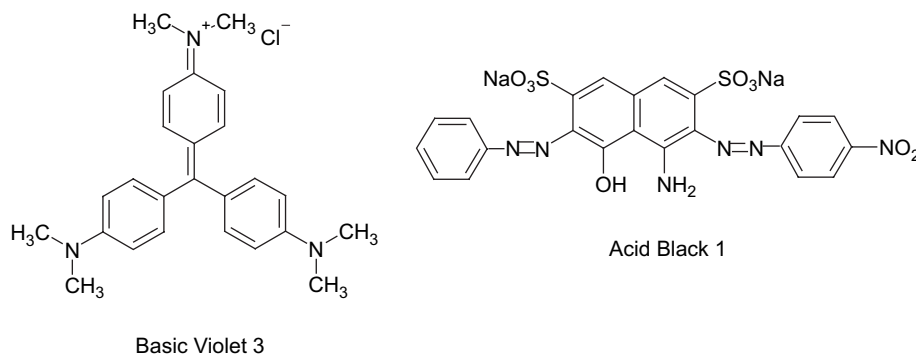


Fig. 1. Chemical structure of investigated dyes.

at different particle sizes and a carbon-enriched sample with particle size $> 150 \mu\text{m}$ was obtained. Secondly, a water washing method was used to get the higher concentrated unburned carbon from the portion of carbon-enriched fly ash.

Two dye samples, Acid Black 1 and Basic Violet 3, were employed for dye adsorption. Their chemical structures are given in Fig. 1. A stock solution with concentration at 10^{-4} M was prepared and the solutions for adsorption tests were prepared from the stock solution to the desired concentration.

The batch kinetic experiments were used to investigate the influence of sorbent mass, solution pH and temperature on the adsorption rate. The adsorption of dyes was performed by shaking 10 mg of solid in 200 ml of dye solution of varying concentration at 100 rpm at different temperatures (Certomat R shaker from B. Braun). The determination of dyes was done spectrophotometrically on a Spectronic 20 Genesis Spectrophotometer (USA) by measuring absorbance at λ_{max} of 618 and 590 nm for Acid Black 1 and Basic Violet 3, respectively. To investigate the effect of pH on adsorption, a series of dye solution was prepared by adjusting pH over a range of 2–11 using 1 M HNO₃ or NaOH solution. The pH of solutions was measured with a pH meter (Radiometer PHM250 ion Analyser).

3. Results and discussion

3.1. Effect of particle size

Fig. 2 presents the dye adsorption on unburned carbon at different particle sizes. As shown, particle size has a significant influence on dye adsorption and a similar variation can be observed for two dyes. Larger particle size of unburned carbon will reduce the adsorption capacity. Several investigations have shown similar observation for activated carbon and other adsorbents [13,15–17]. This relationship indicates that external transport limits the rate of adsorption and powdered adsorbent would be advantageous over granular particles [15].

3.2. Effect of pH

The solution pH will have a significant influence on dye adsorption. Fig. 3 presents the dynamic adsorption of two dyes

on unburned carbon at different solution pH. As shown, adsorption of acid dye exhibits different behaviour with basic one. For Acid Black 1, adsorption decreases with increasing solution pH. This is due to the anion dye reaction with H⁺. Higher pH will produce more OH⁻ ions in solution, preventing the adsorption of dye anions on the adsorbent surface. For Basic Violet, adsorption is higher at pH = 3 than at pH = 6 and adsorption at pH = 9 is the highest. Similar behaviour has also been reported by other researchers [13]. As a basic dye, Basic Violet 3 will produce cation (C⁺) and

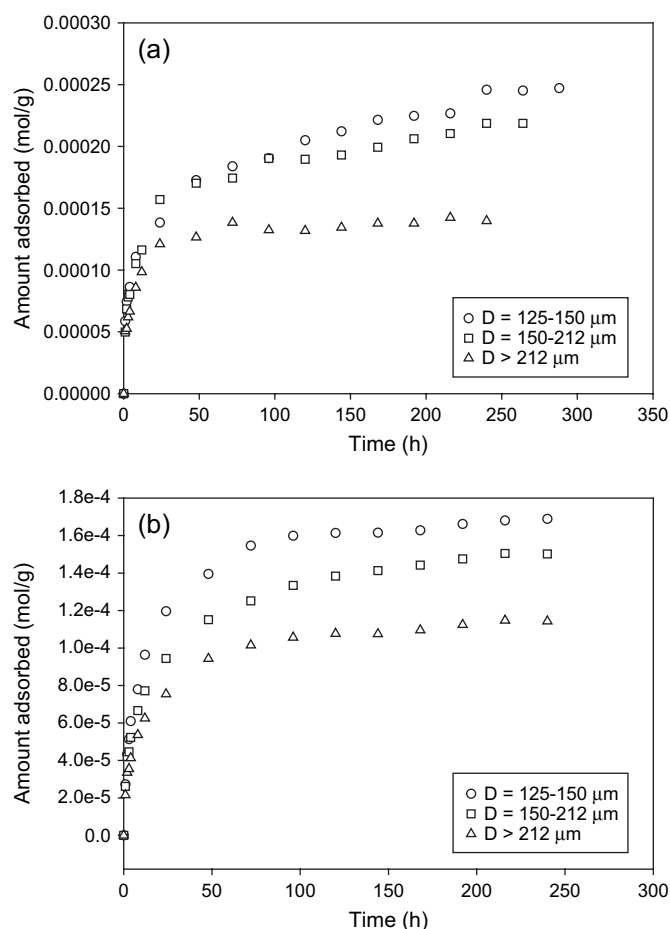


Fig. 2. Effect of particle size on dye adsorption on unburned carbon. (a) Acid Black 1, (b) Basic Violet 3.

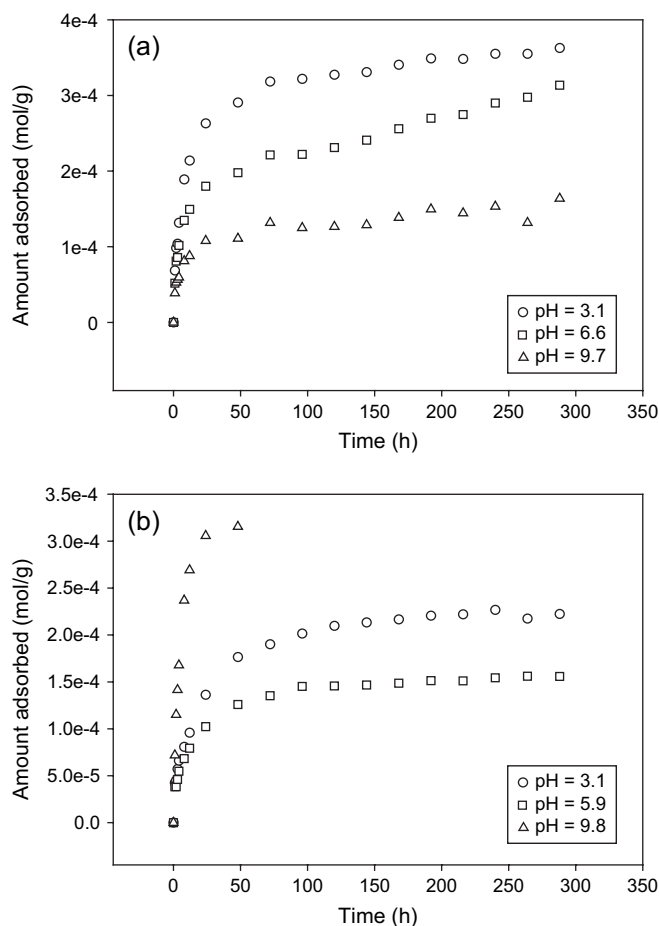


Fig. 3. Effect of solution pH on dye adsorption on unburned carbon. (a) Acid Black 1, (b) Basic Violet 3.

reduced ions (CH^+) in water. As the pH of the dye solution becomes higher, the association of dye cations on solid will take place more easily.

3.3. Effect of temperature

It has been believed that the temperature generally has two major effects on the adsorption process. Increasing the temperature will increase the rate of diffusion of the adsorbate molecules across the external boundary layer and in the internal pores of the adsorbent particle, owing to the decrease in the viscosity of the solution. In addition, changing the temperature will change the equilibrium capacity of the adsorbent for a particular adsorbate [18].

Fig. 4 shows the effect of temperature on dynamic adsorption of two dyes on unburned carbon. It is seen that higher temperature will result in an increase in dye adsorption on unburned carbon, suggesting that the dye adsorption is an endothermic process. The temperature seems to have a significant effect on Acid Black adsorption while less effect on Basic Violet adsorption. For Basic Violet, the adsorption approaches equilibrium after 100 h and the adsorption capacity will reach 2×10^{-4} mol/g at 50 °C. However, for Acid Black, the

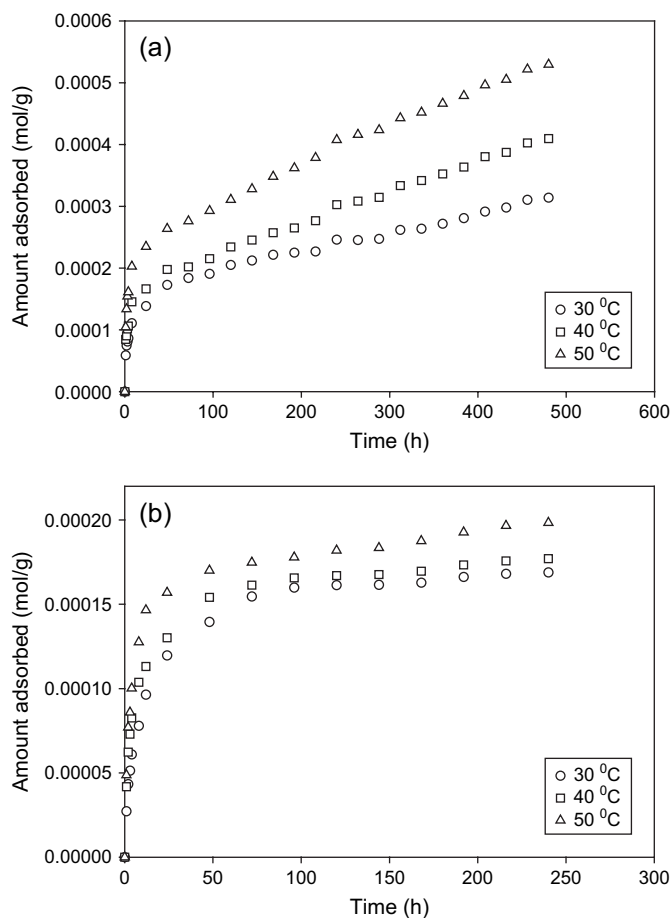


Fig. 4. Effect of temperature on dye adsorption on unburned carbon. (a) Acid Black 1, (b) Basic Violet 3.

adsorption shows gradual increase and no equilibrium will be established after 500 h.

3.4. Kinetic modelling

Most sorption processes take place by a multistep mechanism comprising: (i) diffusion across the liquid film surrounding the solid particles (a process controlled by an external mass transfer coefficient), (ii) diffusion within the particle itself assuming a pore diffusion mechanism (intraparticle diffusion) and (iii) physical or chemical adsorption at a site [3].

The transient behaviour of the batch sorption process at different temperatures was analysed using the Lagergren first-order kinetic model and the pseudo-second-order model [19–21]. The Lagergren first-order model was given by the equation

$$\log(q_e - q_t) = \log q_e - \frac{k_1}{2.303} t \quad (1)$$

where, q_t and q_e represent the amount of dye adsorbed (mol g^{-1}) at any time t and at equilibrium time, respectively, and k_1 represents the adsorption rate constant (h^{-1}). In this

equation, it is necessary to know q_e while it is seen from Fig. 4 that the equilibrium is difficult to achieve. Hence, we use the following equation for curve fitting of the Lagergren first-order kinetic reaction.

$$q_t = q_e (1 - e^{-k_{ad}t}) \quad (2)$$

Figs. 5a and 6a show the fitted curves of different dyes at 30 °C based on Eq. (2). From the figures, it is observed that the sorption data are well represented by the Lagergren model only for the first 20 h for Basic Violet and thereafter it deviates

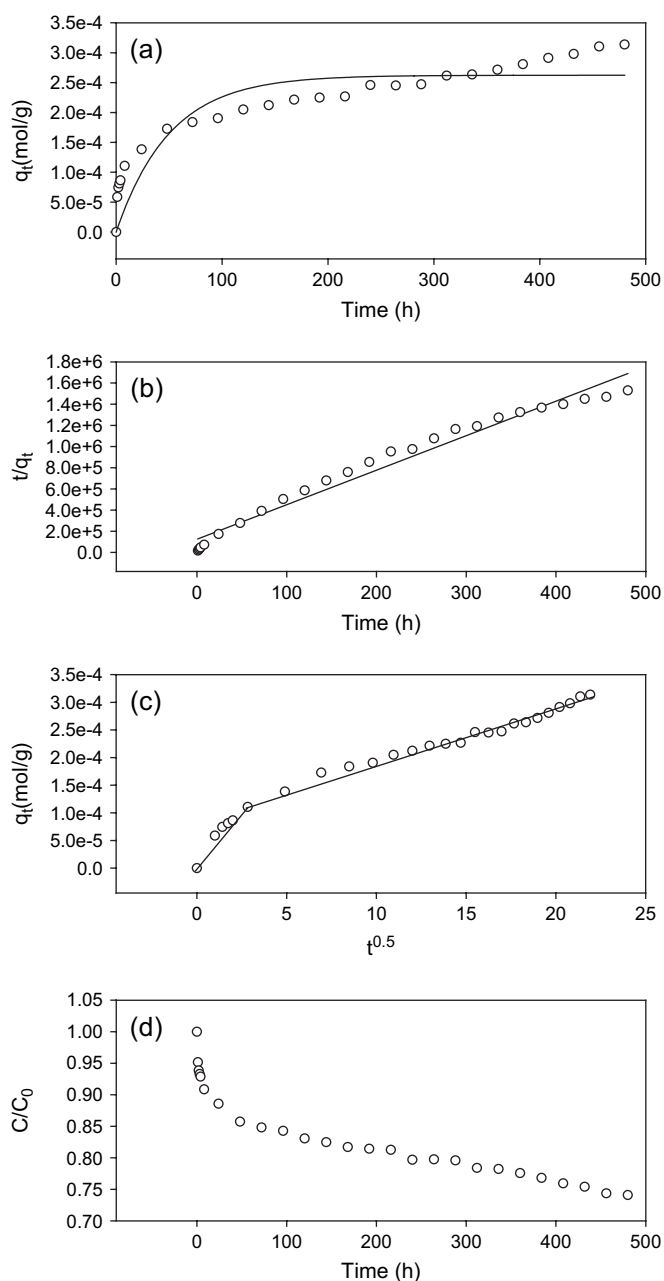


Fig. 5. Comparison of kinetic models of Acid Black 1 on unburned carbon. (a) First-order kinetics, (b) second-order kinetics, (c) intraparticle model, (d) external model.

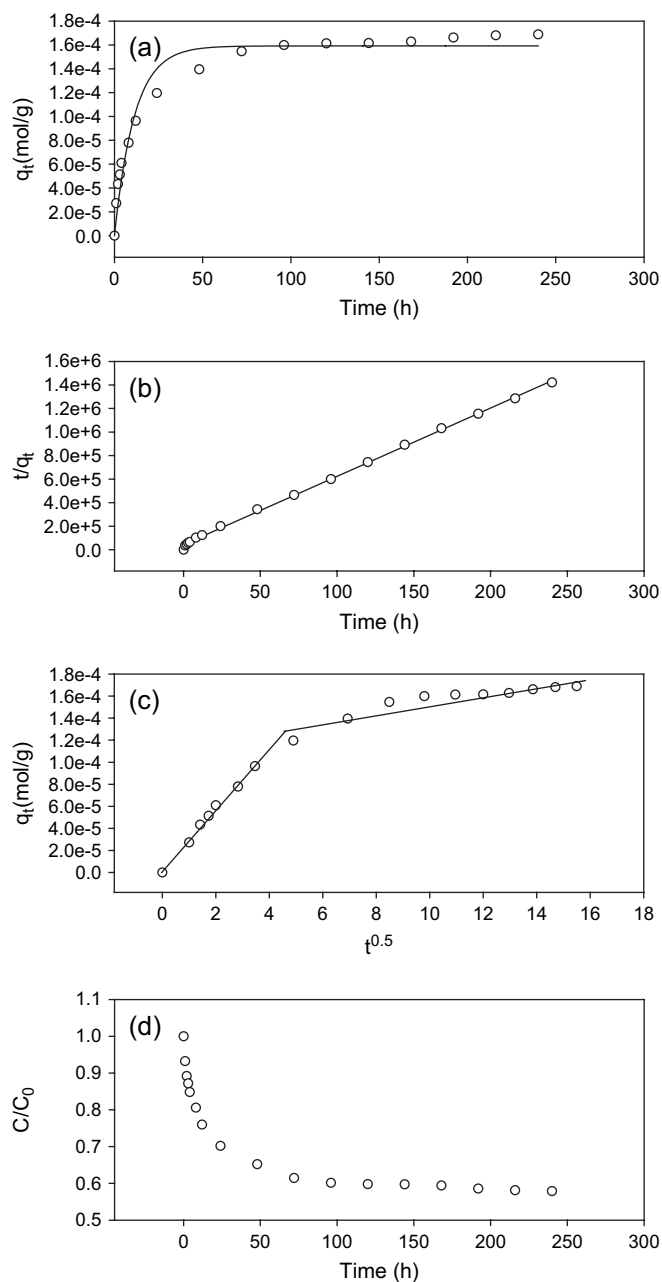


Fig. 6. Comparison of kinetic models of Basic Violet 3 on unburned carbon. (a) First-order kinetics, (b) second-order kinetics, (c) intraparticle model, (d) external model.

from theory and the sorption data cannot be well fitted for Acid Black 1. This confirms that it is not appropriate to use the Lagergren kinetic model to predict the sorption kinetics of two dyes onto the unburned carbon for the entire sorption period. The predicted rate constants using the modified Lagergren equation from Figs. 5a and 6a and their corresponding regression correlation coefficient values are shown in Table 1. As seen from the coefficients, data are less than 0.96 and the equilibrium capacities are lower comparing with the experimental data. It is noted that the first-order kinetic rate is higher for Basic Violet than that of Acid Black.

Table 1
Kinetic parameters obtained from the various models

Dye	First-order kinetics			Second-order kinetics			Intraparticle kinetics	External diffusion model
	k_1 (h ⁻¹)	q_e (mol/g)	R^2	k_2 (g mol ⁻¹ h ⁻¹)	q_e (mol/g)	R^2	k_i (mol/g h ^{1/2})	k_s (h ⁻¹)
Basic Violet	0.0881	1.59×10^{-4}	0.964	772.86	1.72×10^{-4}	0.999	1.88×10^{-6}	0.054
Acid Black	0.0198	2.62×10^{-4}	0.799	85.14	3.07×10^{-4}	0.973	9.45×10^{-6}	0.031

The kinetic data were further analysed using a pseudo-second-order relation, the linear form of which is as follows:

$$\frac{t}{q_t} = \frac{1}{k_2 q_e^2} + \frac{1}{q_e} t \quad (3)$$

where k_2 is the pseudo-second-order rate constant of sorption (g mol⁻¹ h⁻¹), q_e is the amount of dye sorbed (mol g⁻¹) at equilibrium and q_t is the amount of dye on the surface of the sorbent (mol g⁻¹) at any time t . Figs. 5b and 6b present the linear correlation of the pseudo-second-order kinetics for the two dyes. In this study, the kinetic data show a good compliance with this pseudo-second-order equation ($R^2 > 0.970$) and the equilibrium adsorption capacities are close to the experimental data. For the second-order kinetic rate, Basic Violet has higher value than Acid Black, the same as the case for the first-order kinetic model.

From a mechanistic viewpoint, to interpret the experimental data, it is necessary to identify the steps involved during adsorption, described by external mass transfer (boundary layer diffusion) and intraparticle diffusion. According to previous studies, the intraparticle diffusion plot may compose a multilinearity, representing the different stages in adsorption. An intraparticle diffusion model is defined as follows:

$$q_t = k_i(t^{1/2}) \quad (4)$$

where the parameter, k_i (mol/g h^{1/2}), is the diffusion coefficient. In theory the plot between q and $t^{1/2}$ is given by multiple regions representing the external mass transfer followed by intraparticle diffusion in macro, meso, and micropore [3]. From Figs. 5c and 6c it was observed that there were two linear portions, indicating two-stage diffusion of dyes onto unburned carbon particles. The slope of the second linear portion characterises the rate parameter corresponding to the intraparticle diffusion, whereas the intercept of this second linear portion is proportional to the boundary layer thickness. Table 1 gives the values of k_i for two dyes. As seen, acid dye produces the higher diffusion coefficient, resulting in higher adsorption capacity.

As the double nature of the intraparticle diffusion plot suggested the external mass of dye particles at initial time periods, the rate constant corresponding to external mass transfer at these initial time intervals was calculated using the plot of C/C_0 vs time t , where C and C_0 represent the concentration (mol/l) at any time and the initial concentration, respectively. Figs. 5d and 6d show the plots of C/C_0 vs time at 30 °C. The k_s values were obtained using the data before 6 h for linear

regression and are given in Table 1. It is shown that Basic Violet 3 has the higher diffusion rate, leading it to reach equilibrium faster.

In order to determine the actual rate-controlling step involved in the dye sorption process, the sorption data were further analysed using the kinetic expression given by Boyd et al. [3,22]

$$F = 1 - \frac{6}{\pi^2} \exp(-Bt) \quad (5)$$

where F is the fraction of solute adsorbed at different times t and Bt is a mathematical function of F and is given by

$$F = \frac{q_t}{q_e} \quad (6)$$

where, q_t and q_e represent the amount adsorbed (mol/g) at any time t and at infinite time. In this work, we take q_e from the second-order kinetic model. Substituting Eq. (6) in Eq. (5), the kinetic expression becomes

$$Bt = -0.4977 - \ln\left(1 - \frac{q_t}{q_e}\right) \quad (7)$$

Thus the value of Bt can be calculated for each value of F using Eq. (7). The calculated Bt values were plotted against time as shown in Fig. 7. The linearity of this plot will provide useful information to distinguish between external-transport and intraparticle-transport-controlled rates of adsorption [3]. From Fig. 7, it was observed that the plots were not linear,

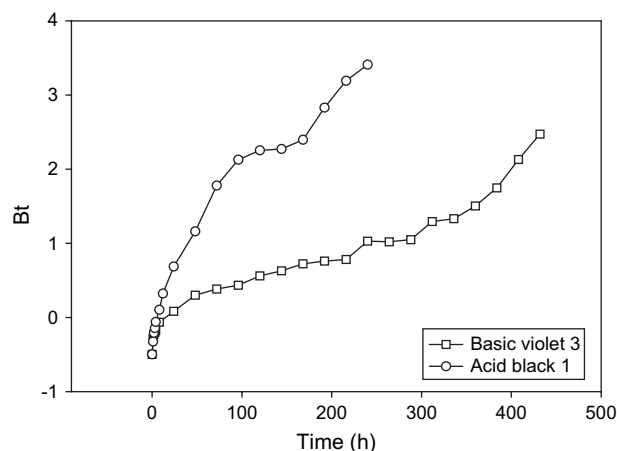


Fig. 7. Boyd plot for Acid Black 1 and Basic Violet 3.

Table 2
Kinetic parameters for Basic Violet and Acid Black obtained at different temperatures

Dye	Temp (°C)	k_2 (g mol ⁻¹ h ⁻¹)	q_e (mol/g)	R^2	k_i (mol/g h ^{1/2})	Layer thickness (mol/g)	k_s (h ⁻¹)
Basic Violet	30	772.86	1.72×10^{-4}	0.964	1.88×10^{-6}	1.40×10^{-4}	0.054
	40	1027.65	1.78×10^{-4}	0.999	2.44×10^{-6}	1.39×10^{-4}	0.075
	50	981.78	1.97×10^{-4}	0.998	3.64×10^{-6}	1.42×10^{-4}	0.093
Acid Black	30	85.14	3.07×10^{-4}	0.973	9.45×10^{-6}	9.74×10^{-5}	0.031
	40	47.92	4.05×10^{-4}	0.952	1.40×10^{-5}	8.68×10^{-5}	0.035
	50	41.20	5.27×10^{-4}	0.963	1.76×10^{-5}	1.32×10^{-4}	0.052

indicating that external mass transport mainly governs the rate-limiting process. This is confirmed by the observation in the adsorption at different particle sizes.

Table 2 presents the parameters obtained from the various kinetic models at different temperatures. As seen, the adsorption equilibrium capacity increases with the increasing temperature for both dyes and that unburned carbon presents higher adsorption capacity for Acid Black. The pseudo-second-order kinetic rate constant, k_2 , shows different trend variation for the two dyes. For Basic Violet, k_2 increases as the temperature increases from 30 to 40 °C and then it keeps close to the value at 50 °C, indicating that the adsorption mechanism is different at higher temperature from that at lower temperature. The diffusion rates for intraparticle and external diffusion also show an increasing trend with the temperature due to the endothermic characteristics of diffusion process. On the other hand, the pseudo-second-order kinetic rate constant for Acid Black adsorption shows a decreasing trend with the temperature, suggesting that the chemical process is an exothermic reaction. While the diffusion rates for intraparticle and external diffusion processes are increasing with the increasing temperature, similar to the basic dye adsorption. These also demonstrate that diffusion process for acid dye is also an endothermic process.

From the kinetic parameters, k_2 , k_i and k_s at varying temperatures, the activation energies for the three processes can be estimated and their values are presented in Table 3. As shown, the activation energies from the pseudo-second-order kinetics for acid and basic dyes are different. The negative value of the activated energy for acid dye indicates that the adsorption is not a chemical but a physical process while the positive values of activated energies for basic dye indicate that the adsorption process is a combination of chemical and diffusion processes. Although the activated energy for basic dye is positive, it is much lower compared with the values of two diffusion processes. This confirms that diffusion process is the control step for adsorption. The data in Table 3 also show that the activated energy for the intraparticle diffusion is higher than that of external

diffusion for both dyes and the activated energies for Basic Violet are higher than those of Acid Black, resulting in higher adsorption capacity of acid dye than that of Basic Violet.

4. Conclusion

Dynamic adsorption of acid and basic dyes on unburned carbon derived from coal fly ash has been conducted in aqueous solution. Several adsorption parameters such as adsorbent particle size, solution pH and temperature have been investigated. Several kinetic models have been employed to model the adsorption mechanism. It is found that the sorption dynamic data followed the pseudo-second-order kinetics. Two mechanisms including external diffusion and intraparticle diffusion play roles in adsorption process and the dominating process was found to be the external diffusion control. For Basic Violet, the adsorption involves both physical and chemical processes while the adsorption is the main process for the Acid Black.

References

- [1] Hao OJ, Kim H, Chiang PC. Decolorization of wastewater. *Crit Rev Environ Sci Technol* 2000;30:449–505.
- [2] Reife A, Freeman HS. Pollution prevention in the production of dyes and pigments. *Text Chem Color Am Dyes Rep* 2000;32:56–60.
- [3] Kumar KV, Ramamurthi V, Sivanesan S. Modeling the mechanism involved during the sorption of methylene blue onto fly ash. *J Colloid Interface Sci* 2005;284:14–21.
- [4] Walker GM, Hansen L, Hanna J-A, Allen SJ. Kinetics of a reactive dye adsorption onto dolomitic sorbents. *Water Res* 2003;37:2081–9.
- [5] Wang SB, Boyjoo Y, Choueib A, Zhu ZH. Removal of dyes from aqueous solution using fly ash and red mud. *Water Res* 2005;39:129–38.
- [6] Hsieh YM, Tsai MS. Physical and chemical analyses of unburned carbon from oil-fired fly ash. *Carbon* 2003;41:2317–24.
- [7] Wang SB, Boyjoo Y, Choueib A, Ng E, Wu H, Zhu Z. Role of unburnt carbon in adsorption of dyes on fly ash. *J Chem Technol Biotechnol* 2005;60:1401–7.
- [8] Serre SD, Silcox GD. Adsorption of elemental mercury on the residual carbon in coal fly ash. *Ind Eng Chem Res* 2000;39:1723–30.
- [9] Zhang YZ, Lu Z, Maroto-Valer MM, Andresen JM, Schobert HH. Comparison of high-unburned-carbon fly ashes from different combustor types and their steam activated products. *Energy Fuels* 2003;17:369–77.
- [10] Gupta VK, Mohan D, Sharma S, Sharma M. Removal of basic dyes (rhodamine B and methylene blue) from aqueous solutions using bagasse fly ash. *Sep Sci Technol* 2000;35:2097–113.
- [11] Janos P, Buchtova H, Ryznarova M. Sorption of dyes from aqueous solutions onto fly ash. *Water Res* 2003;37:4938–44.

Table 3
Activation energies of dye adsorption on unburned carbon

Dye	E_{a-k_2} (kJ/mol)	E_{a-k_i} (kJ/mol)	E_{a-k_s} (kJ/mol)
Basic Violet 3	9.9	26.8	22.2
Acid Black 1	−29.7	25.4	20.9

- [12] Khare SK, Panday KK, Srivastava RM, Singh VN. Removal of Victoria blue from aqueous solution by fly ash. *J Chem Technol Biotechnol* 1987;38:99–104.
- [13] Mohan D, Singh KP, Singh G, Kumar K. Removal of dyes from wastewater using flyash, a low-cost adsorbent. *Ind Eng Chem Res* 2002;41:3688–95.
- [14] Ramakrishna KR, Viraraghavan T. Dye removal using low cost adsorbents. *Water Sci Technol* 1997;36:189–96.
- [15] Gupta VK, Ali I, Suhas, Mohan D. Equilibrium uptake and sorption dynamics for the removal of a basic dye (basic red) using low-cost adsorbents. *J Colloid Interface Sci* 2003;265:257–64.
- [16] Dogan M, Alkan M, Onganer Y. Adsorption of methylene blue from aqueous solution onto perlite. *Water Air Soil Pollut* 2000;120:229–48.
- [17] Ozacar M, Sengil IA. Adsorption of reactive dyes on calcined alunite from aqueous solutions. *J Hazard Mater* 2003;98:211–24.
- [18] Al-Qodah Z. Adsorption of dyes using shale oil ash. *Water Res* 2000;34:4295–303.
- [19] Ho YS, McKay G. Kinetic models for the sorption of dye from aqueous solution by wood. *Process Saf Environ Prot* 1998;76:183–91.
- [20] Ho YS, McKay G. Pseudo-second order model for sorption processes. *Process Biochem* 1999;34:451–65.
- [21] Ho YS, Chiang CC. Sorption studies of acid dye by mixed sorbents. *Adsorption* 2001;7:139–47.
- [22] Gupta VK, Ali I. Removal of DDD and DDE from wastewater using bagasse fly ash, a sugar industry waste. *Water Res* 2001;35:33–40.